Evaluation of metal contamination in surface sediments and macroalgae in mangrove and port complex ecosystems on the Brazilian Equatorial Margin

Marco Valério Jansen Cutrim (marco.cutrim@ufma.br)
Universidade Federal do Maranhao https://orcid.org/0000-0002-7442-2121
James Jordan Marques Corrêa
Universidade Federal do Maranhão: Universidade Federal do Maranhao

Research Article

Keywords: Brazilian Equatorial Margin, mangrove ecosystem, surface sediment contamination, metal accumulation

Posted Date: May 20th, 2022

DOI: https://doi.org/10.21203/rs.3.rs-1505643/v1

Abstract

This study evaluated metal contamination in surface sediments and macroalgae of mangroves and port complexes on the Brazilian equatorial margin. Samples were collected between August 2020 and February 2021 at seven points in a mangrove swamp under the influence of port activity and at two points without port activity. Metal concentrations in the macroalgae and sediments were determined using inductively coupled plasma optical emission spectrometry. All macroalgal species bioaccumulated metals, as demonstrated by their bioaccumulation factors. The geochemical contamination indices indicated that the estuarine complex was influenced by port activity as moderately contaminated by Pb, Cr, Mn, and Fe, and considerably contaminated by Zn and Cu. The enrichment factor confirmed significant mineral enrichment of Zn and Cu in this environment. The concentrations of the metals in the sediment followed the order Fe > Mn > Cr > Zn > Cu > Pb at most collection points. *Cladophoropsis membranacea* recorded the highest bioaccumulation values for Pb (0.44), *Rhizoclonium africanum* for Zn (1.08), Cr (0.55), and Fe (0.30), an*d Bostrychia radicans* for Mn (2.22). The bioaccumulation pattern of metals in the most abundant macroalgal species followed the order *Bostrychia radicans* (Mn > Zn > Cu > Cr > Pb > Fe) and *Rhizoclonium africanum* (Zn > Mn > Cr > Cu > Pb > Fe).

Introduction

Globally, coastal regions undergo significant environmental stresses and are under pressure from various forms of anthropogenic activity. In this century alone, 80% of human activity has been concentrated in coastal zones (GRUBER et al. 2003). Intense urbanization, tourism, port use, and industrial activity are examples of large-scale human interventions within coastal regions. Most mangrove extensions of the South American Eastern margin (approximately 80%) occur along the Brazilian coast (Ferreira and Lacerda 2016). Mangroves cover large areas in Brazil, with a patchy distribution along the 6,800 km coastline. The most extensive mangrove areas are in the north—Amapá State, Pará State, and Maranhão State—with wide tidal ranges and high levels of rainfall, which encourage their development. As this ecosystem preferentially develops in coastal areas, mangroves continuously undergo numerous interventions. According to Neumann et al. (2015), high rates of population growth and urbanization in coastal regions are likely to persist. This rapid and disorganized urban expansion has a significant impact on mangroves. Among anthropogenic impacts, we highlight the release of domestic and industrial sewage, mining, indiscriminate use of agricultural fertilizers and pesticides, and harbor activities. These activities are potentially harmful to estuaries and, consequently, mangroves and the organisms that depend on them. Metals are the most abundant contaminants resulting from these activities. Metals can enter the aquatic environment in the following forms: dissolved (in the water column and interstitial water of the sediments), particulate (linked to the suspended material and bottom sediment) (Yahya, Mohamed and Mohamed 2018), and biotic absorption. Non-degradable substances, such as metals, are observed at the same time toxicity, persistence, and bioaccumulation in the food chain (Marcovecchio 2000; Marins et al. 2002), which makes it relevant to study the absorption of such elements by primary producers, which

are the basis of the trophic chain, such as macroalgae. Macroalgae are benthic photosynthetic organisms that are closely related to nutrient cycling in the environment where they occur. They act as the basis of the food chain because they are primary producers that play a fundamental role in ecological structure, functioning, and balance while serving as an essential renewable resource within marine ecosystems (Valentin 2010). In mangroves, macroalgae attach themselves to various substrates such as roots, pneumatophores, dead branches, trunks, and muddy surfaces (Dawes et al. 1999). The use of macroalgae as biomonitoring organisms has been increasing in metal contamination assessments (Billah et al. 2017; Taylor et al. 2017; Reis et al. 2016; Chakraborty et al. 2014). These organisms provide key information due to their high capacity to accumulate toxic substances, which allows their use as a tool for quantitatively assessing their environment. Therefore, they are called biological sponges, whose substance capture is controlled by two factors (Baoli and Congqiang 2004). The first factor is the environment and is influenced by metal concentrations. The second is the biological factor and is influenced by macroalgal affinity for metals. Such metals can enter these organisms in two ways: adsorption on their extracellular walls (biosorption) or absorption inside the cell (bioaccumulation) (Veglio and Beolchini 1997). Studies have shown that the effect of each metal on algae depends on factors such as the type of metal, concentration, and exposure time (Mamboya et al. 1999) in addition to the chelation and detoxification levels of each alga (Lombardi and Vieira 1998). In Brazil, studies of macroalgae as biomonitors of metal contamination have been conducted in Rio de Janeiro (Lacerda et al. 1985; Karez et al. 1994; Amado Filho et al. 1999; Machado et al. 2003), Pernambuco (Macedo et al. 2009) and Bahia (Brito et al. 2012). Overall, few studies have reported biomonitoring of metal contamination using macroalgae from mangrove ecosystems. However, the accumulation patterns of metals in the mangroves of the Brazilian equatorial margin and port areas have not yet been determined. Therefore, studying estuarine environments and mangroves on the equatorial margin of Brazil using sediment and macroalgae is of great importance because the region has the longest continuous band of mangroves in the country. This ecosystem partially includes one of the most important port areas on the north coast of Brazil, which has been recognized for the intensive movement of iron and manganese minerals that occurs in the region. Port activities are potential sources of contamination in coastal ecosystems (Jahan and Strezov 2019; Buruaem et al. 2012; Shafie et al. 2012; Hortellani and Sarkis, 2008). The contamination that occurs around ports can compromise the ecosystem services provided by mangroves as the organisms that inhabit this environment are food and income sources for many communities around the world. The present study focused on (1) determining the metal levels (Cu, Zn, Fe, and Mn) in sediment in the study area; (2) investigating the patterns of metal accumulation in the dominant mangrove macroalgal species associated with pneumatophores and tree trunks of mangroves; and (3) determining the geo-accumulation index (Igeo), contamination factor (CF), enrichment factor (EF), and pollution load index (PLI). An assessment of metal concentrations in this region is necessary to identify the vulnerability of these ecosystems to pollution and compile baseline data for future monitoring.

Material And Methods

Study area

The study area comprises two large estuarine systems on the Brazilian equatorial margin with recognized importance for the region: the São Marcos estuarine complex (SMEC) and the São José complex (SJEC).

The Itaqui Port Complex (IPC) is located at the SMEC, which has been internationally recognized for its operational capacity. The IPC comprises the Itaqui Organized Terminal (IOT), Ponta da Espera Maritime Terminal (PEMT), and Alumar Private Use Terminal (PUT Alumar). Intensive movement of solid mineral bulk consisting of iron and manganese ores occurs in the PEMT (MTPA, 2018). PUT Alumar is responsible for handling bauxite and alumina loads (MTPA, 2018). The processing of bauxite generates as a by-product the so-called red mud consisting of iron, aluminum, sodium, and calcium oxides, as well as titanium dioxide and metals such as gallium, vanadium, and rare earth.

SJEC was marked by intense urbanization, mainly at points 09 and 08. However, there was little to no industrial activity, especially in the absence of port activity.

Due to the strong fluvial input in both estuarine complexes, the waters are characteristically turbid, with high concentrations of particulate matter, mainly clay and silt, originating from continental and mangrove areas (Silva, 2011).

The region's climate is tropical, marked by well-defined periods of rain and drought, with an average annual rainfall of 1,896 mm/year and an average temperature of 27 °C (https://www.climatempo.com.br). Thus, it is part of the context of humid tropical regions between 15°N and 15°S latitude, whose characteristics are high and constant precipitation (> 1,500 mm/year), temperatures > 20°, and low thermal variation (Nittrouer et al., 1995).

Because of these characteristics, the study area is characterized by the presence of structurally complex mangroves (Rebelo-Mochel 1997), the most abundant of which are *Rhizophora mangle* Linnaeus (1753), *Avicennia germinans* (L.) Stearn (1958), and *Laguncularia racemosa* (L.) CF Gaertn.

Sediment and macroalgae sampling

Sampling was conducted between August 2020 and February 2021 at nine sampling points: P01 to P07 in SMEC and P08 and P09 in SJEC (Fig. 1).

At all points, the in-situ water temperature, pH, salinity, total dissolved solids (TDS), and dissolved oxygen (DO) were determined using a multiparametric probe model HANNA HI 98194.

The intertidal surface sediments (top 5 cm) were collected using a plastic scoop at each sampling point. Three replicates of each sample were conducted in each plot of the study area (n = 54; considering two sample surveys). The sediment samples were dried in the laboratory at 60^{o}C for 48 h and ground for further treatment.

Macroalgae were collected from the trunks and pneumatophores in the intertidal zone at each sampling point. Five pneumatophores were randomly harvested from a single sampling plot and cut in the mudline using a clipper (Billah et al. 2017). Therefore, 90 pneumatophores (45 pneumatophores × 2 samples) were harvested. In the laboratory, the samples were carefully washed to remove adhered particles and identified based on marine macroalgae literature (JHA et al. 2009).

Determination of metal concentrations in macroalgae

In the laboratory, the algae samples were lyophilized at -20 °C for 48 h, crushed, and homogenized for the additional procedures. Extraction of inorganic elements from macroalgae was performed using 0.750 g (dry weight) of the crushed sample. Initially, the lyophilized samples were placed in Teflon tubes (X-press) to which concentrated HNO_3 (8 ml) and concentrated HF (2 mL) were added.

The extracts were allowed to rest overnight at room temperature and then placed in a microwave, model Mars X-press (CEM), for 40 min (15 min –ramp and 25 min–wait) at a temperature of 175 °C and power of 1600 W, adapted from EPA 3052. After cooling (30 min), H_3BO_3 (12 mL) was added to neutralize the HF, and then the tubes were taken back to the microwave for 25 min (15 min, ramp and 10 min, hold) at 170 °C.

The final cooled extract was filtered (Whatman No. 40) and measured at a final volume of 25 mL with 0.5 N HNO_3 in a volumetric flask. The elements were determined using inductively coupled plasma optical emission spectrometry (IPC-OES 720). Precision measurements were obtained from the digestion of macroalgae and sediment in triplicate every 10 samples, and accuracy was determined from certified macroalgae and sediment standards Apple Leaves NIST SRM 1515. Recovery rates for metals in the macroalgae were 106% for Zn, 92.7% for Cu, 99.6% for Cr and 104.5% for Fe.

Elementary extraction and determination of metals in sediment

Initially, dried and powdered sediment (0.5 g) was placed in Teflon tubes (X-press) to which HNO_3 (9 ml), HF (4 ml), and HCl (2 ml) were added. The extracts were allowed at rest overnight at room temperature and then placed in a microwave, model Mars X-press (CEM), for 40 min (15 min - Ramp and 25 min - waiting) at a temperature of 175 °C and power of 1600 W. These adjustments were adapted from a method described by the United States Environmental Protection Agency (EPA 3052). After cooling (30 min), H_3BO_3 (25 mL) was added to neutralize the HF, and the tubes returned to the microwave where they remained for 25 min (15 min, ramp and 10 min, hold) at 170 °C. After cooling for 30 min, the final extract was filtered (Whatman No. 40) and measured at a final volume of 50 mL with 0.5 N HNO_3 in a volumetric flask. The determination of metals was performed later in the IPC-OES 720 equipment, and NIST 1646a was used as the standard. Recovery rates for metals in the sediment were 98% for Zn, 92% for Cu, 111% for Pb, 95% for Cr, 94% for Mn, and 95% for Fe. All analyses were performed in triplicate.

Granulometric analysis and Pejrup diagram

An interval-programmed Sald-3101 Shimadzu laser diffraction particle analyzer (Table 1) was used to determine the particle size using an aliquot of 2 g of the crude sample.

Table 1 Ranges of granulometric values according to the Wentworth classification (1922)

Phi	Wentworth Classification	Diameter
0	very coarse sand	2mm - 1mm
1	coarse sand	1mm - 500µm
2	medium sand	500µm - 250µm
3	thin sand	250 µm - 125µm
4	very thin sand	125µm-63µm
5	coarse silt	63µm - 31µm
6	medium silt	31µm - 16µm
7	fine silt	16µm - 8µm
8	very fine silt	8µm - 4µm
9	clay	< 4µm

The particle size distribution was treated using the SYSGRAN program (version 3.0), producing the following parameters: mean, median, standard deviation, asymmetry, kurtosis, normalized kurtosis, Wentworth classification, selection degree, and kurtosis classification. The statistical parameters of the particle size distributions were calculated from the particle size diameters (fi, mean, median, standard deviation, asymmetry, and kurtosis) using the equations proposed by Folk and Ward (1957).

The values obtained from the particle size analysis were used to construct a Pejrup diagram (1988). This diagram indicates the hydrodynamic conditions of the environment based on the sand, silt, and clay content present in the sampled sediment. A higher percentage of grains in the fine fraction indicates calmer hydrodynamic conditions.

The triangular diagram has four hydrodynamic sections (I to IV) that indicate hydrodynamic conditions: low (I), moderate (II), high (III), and very high (IV). In addition, constant sand content lines are suitable for textural classification. Thus, the triangle was divided into four texture classes, indicating a decrease in the sand content in the sediment. The sand percentages ranged from A to D, with A (90–100%), B (50–90%), C (10–50%), and D (0–100%).

Geo-accumulation index (Igeo), contamination factor (CF), enrichment factor (EF), and pollution load index (PLI)

The geochemical background values for Zn, Cu, Pb, Cr, Mn, and Fe proposed by De Paula Filho et al. (2015) in a study carried out in the Parnaíba Delta were used to calculate the indices. The São Luís Island and Parnaíba sedimentary basins are classified in the same morphological unit type, known as the Barreiras do Tertiary Group (CPRM 2000).

Fe was adopted as a reference element because of its similarity to other trace metals, uniform natural concentration, and its characteristic association with thin solid surfaces (Varol 2011). Thus, it was considered suitable as a normalizing element for the evaluated indices.

Geo-accumulation index (Igeo)

This index quantifies the metal pollution in aquatic sediments (Muller, 1979) using the following formula:

$$I_{geo} = Log_2 C_N/1{,}5B_N$$

where CN is the concentration of the “N” element measured in the sediment, 1.5 is a correction factor for the background matrix that includes any possible variations in values due to lithogenic effects (Muller 1979), and BN is the background value of the element (Zhiyuan et al. 2011; Ozkan 2012). Below, seven descriptive classes were proposed for the values obtained from the geo-accumulation index (Table 2).

Table 2 Geo-Accumulation Index (Igeo) classes and values for sediment quality

I_{geo} Value	I_{geo} Class	Sediment Quality
0	0	Uncontaminated
0 – 1	1	Uncontaminated to Moderately Contaminated
1 – 2	2	Moderately Contaminated
2 – 3	3	Moderately to strong contaminated
3 – 4	4	Strongly contaminated
4 – 5	5	Strongly to Extremely contaminated
> 5	6	Extremely contaminated

Contamination factor (CF)

Hakanson (1980) proposed contamination factor (CF) as a marker to assess the level of metal concentrations in soils. CF corresponds to the ratio between the concentration of metals measured in the sediments and the background value of the metal at a given location (Turekian and Wedepohl, 1961).

$$CF_n = \frac{C_n}{B_n}$$

Where for the "N" element, CF_N is the ratio between the concentration of the element in the sediment (C_N) and the background value (B_N). Using the classification of Hakanson (1980), we obtain:

FC < 1: Low Contamination

1 ≤ FC < 3: Moderate Contamination

3 ≤ FC < 6: Considerable Contamination

FC ≥ 6: High Contamination

Enrichment factor (EF)

The enrichment factor (EF) corresponds to the standardization of a tested element with a reference element (Fe) that has low occurrence variability. The most common reference elements are Sc, Mn, Ti, and Al (Reimann and De Caritat, 2000; Sutherland, 2000).

$$EF = (M_s/Fe_s)/(M_b/Fe_b)$$

Ms and Mb are the concentration of a given metal in the sediment and its background value, respectively. Fes and Feb are the concentration in the sediment and the background value of the reference metal Fe, respectively. The Enrichment Factor has seven categories (Taylor 1964) which are interpreted as:

EF < 1: No Mineral Enrichment;

EF = 1 – 3: Minimum Enrichment

EF = 3 – 5: Moderate Enrichment

EF = 5 – 10: Significant Enrichment;

EF = 10 – 25: Severe Enrichment;

EF = 25 – 50: Very Severe Enrichment;

EF > 50: Extreme enrichment.

EF values ranging between 0.5 and 1.5 suggest the contribution of the crust as a metal source, while values > 1.5 indicate anthropogenic influence (Nowrouzi and Pourkhabbaz 2014).

Pollution load index (PLI)

The Pollution Load Index (PLI) is obtained by multiplying the previously calculated contamination factors (CFs) and subsequent extraction of the root, according to the following equation:

$$PLI = \sqrt[n]{C_f^1 \, x \, C_f^2 \, x \, C_f^3 \, \ldots \, C_f^n}$$

Where: **PLI < 1** No Polluted

PLI = 0 Normal levels

PLI > 1 Polluted Environment

Bioconcentration factor (BCF)

Bioconcentration is the accumulation of contaminants in aquatic organisms through non-dietary absorption pathways, for example, from the soluble phase. The bioconcentration factor has been used to assess the potential for metal bioaccumulation (Conti and Cecchetti 2003; Akcali and Kucuksezgin 2011). The calculation corresponds to the ratio of the metal concentration in the macroalgae to that in the sediment (BCFs) according to the following formula:

$$BCF_s = \frac{C_{macroalgae}}{C_{sediment}}$$

Threshold effect level (TEL), probable effect level (PEL), effects range low (ERL), and effects range medium (ERM)

TEL and PEL are interpretive toxicity criteria for marine and estuarine sediments that were established by Canadian legislation based on compiled biological and chemical data from laboratory studies, field measurements, and numerous models. TEL indicates the level below which there are no adverse effects on the biological community, and PEL is the level above which adverse effects are expected. The range above the TEL and below the PEL represents a possible adverse effect on the community (Hortellani et al. 2008; De Paula Filho et al. 2021).

ERL and ERM are American criteria established by Long et al. (1995) using chemical and biological data from field studies in marine and estuarine sediments. The ERL is the concentration limit below which it is rarely toxic. The ERM, in turn, is the limit above which there is a high likelihood of toxicity, and the range between the ERL and ERM indicates possible toxicity (Hortellani et al. 2008; Long et al. 1995). The ERL

and ERM limits were adopted as reference values by resolutions 344/2004 and 454/2012 of the National Environmental Council (CONAMA, Brazil) for estuarine and marine sediments. The TEL, PEL, ERL, and ERM limits are not applicable to Al, Fe, and Mn.

Table 3 TEL, PEL, ERL and ERM limits for the metals Cd, Cr, Cu, Hg, Ni, Pb and Zn in estuarine and marine sediments. [1]Hortellani et al, 2008; [2]Long et al. 1995

Elements	[1]TEL ($\mu g\ g^{-1}$)	[1]PEL ($\mu g\ g^{-1}$)	[2]ERL ($\mu g\ g^{-1}$)	[2]ERM ($\mu g\ g^{-1}$)
Cd	0.7	4.21	1.2	9.6
Cr	52.3	160	81	370
Cu	18.7	108	34	270
Hg	0.13	0.70	0.15	0.71
Ni	15.9	42.8	20.9	51.6
Pb	30.2	112	46.7	218
Zn	124	271	150	410

Statistical Analysis

The Shapiro-Wilk test was used to verify the normality of all data. ANOVA (One-way) and Kruskal-Wallis tests were used to test for significant differences. Spearman's correlation coefficient was used to understand the paired relationships between the measured variables. For all tests, values of $p < 0.05$ and $p < 0.01$ were considered to indicate statistical significance. Analyses were performed using SPSS v26 software.

Results

Physical and Chemical Variables

The physical and chemical data obtained during sampling are summarized in Table 4. Water temperature, salinity, and dissolved oxygen showed significant differences between the collection points (ANOVA, $p < 0.05$) and TDS (Kruskal-Wallis, $p < 0.05$).

Table 4 Physical and chemical variables of the sampling points (mean $\pm$ standard deviation). Different superscript letters in the same column indicate significant differences between sampling points according to Tukey's Post-Hoc test ($p < 0.05$)

Points	Temperature	Salinity	DO (mg/L)	pH	TDS (g/L)
P01	33.00 ± 1.41^{b}	28.60 ± 0.71^{d}	$7.55 \pm 1.20^{c,e}$	7.55 ± 0.49	$22.35 \pm 0.49^{b,d,e,f,g}$
P02	35.60 ± 0.14^{c}	23.80 ± 0.85^{b}	$6.10 \pm 0.28^{a,e}$	7.30 ± 0.00	$18.95 \pm 0.64^{a,e}$
P03	35.10 ± 0.00^{c}	28.30 ± 0.00^{d}	9.40 ± 0.00^{d}	8.15 ± 0.00	$22.80 \pm 0.00^{d,e,f,g}$
P04	35.05 ± 0.21^{c}	23.63 ± 0.10^{b}	3.46 ± 0.01^{b}	7.80 ± 0.14	$18.92 \pm 0.03^{a,d}$
P05	30.25 ± 0.35^{a}	25.99 ± 0.01^{c}	$6.29 \pm 0.02^{a,c}$	7.78 ± 0.00	$20.30 \pm 0.00^{a,f}$
P06	$31.76 \pm 0.11^{a,b}$	23.09 ± 0.04^{b}	2.27 ± 0.01^{b}	7.85 ± 0.21	$18.40 \pm 0.02^{a,b}$
P07	31.00 ± 0.28^{a}	17.90 ± 0.99^{a}	5.80 ± 0.14^{a}	7.75 ± 0.21	14.65 ± 0.78^{a}
P08	$30.00 \pm 0.00^{a,d}$	26.00 ± 0.00^{c}	$1.55 \pm 0.01^{b,f}$	6.26 ± 0.01	$45.20 \pm 0.00^{f,g}$
P09	28.14 ± 0.06^{d}	$26.85 \pm 0.07^{c,d}$	0.47 ± 0.02^{f}	7.70 ± 0.00	$21.10 \pm 0.00^{a,g}$

The lowest and highest value mean water temperatures were observed in P09 and P02, at 28.14 and 35.60 °C, respectively. P02 (35.60 + 0.14 °C), P03 (35.10 + 0.00 °C), and P04 (35.05 + 0.21 °C) were similar to each other, however, different from all others sampling points (ANOVA, $p < 0.05$).

The mean salinity ranged from 17.9 and 28.6, and the lowest values were found at the collection points belonging to the SMEC. P07 (17.9) showed statistically significant differences compared to all other sampling points (ANOVA, $p < 0.05$).

Macroalgae

In the studied area, 03 species belonging to the Chlorophyceae group, *Cladophoropsis membranacea* Børgesen,1905, *Rhizoclonium africanum* Kutzing, 1853, and *Rhizoclonium tortuosum* Kutzing,1845 and 02 belonging to the Rhodophyceae group, *Bostrychia radicans* Montagne, 1842 and *Catenella caespitosa* Parke and Dixon, 1976, were identified. *R.africanum* was present at all sampling points, except in P05. The second most common species found was *B. radicans*, absent only in P02 and P05. *C.caespitosa* occurred in P1, P4, P6, P8, and P9, *C. membranacea* in P1, P3, P4, P5, and P6, while *R.tortuosum* was found only in P08.

Granulometric analysis and Pejrup diagram

The granulometric analysis recorded mean Phi values between 2.84 and 8.28, showing that the local particle size ranged from medium sand to very fine silt. Sedimentary grains ranged from very poorly to moderately selected, characterizing a variation in particle size between collection points (Table 5).

Most sampling points presented platykurtic or mesokurtic kurtosis with heterogenous value distribution, except for P05 and P08, which recorded leptokurtic kurtosis; these data were concentrated around the mean (Table 5).

Table 5 Particle size analysis of sampled points in the mangroves of São Luís Island, MA

Points	Medio Phi	Wentworth Classification	Selection Degree	Kurtosis
P01	2.84	Medium Sand	Poorly selected	Platykurtics
P02	6.55	Medium Silt	Poorly selected	Platykurtics
P03	6.36	Medium Silt	Moderately selected	Mesokurtics
P04	4.21	Very Fine Sand	Very Poorly selected	Platykurtics
P05	8.28	Very Fine Silt	Moderately selected	Leptokurtics
P06	8.10	Very Fine Silt	Moderately selected	Mesokurtics
P07	8.25	Very Fine Silt	Moderately selected	Mesokurtics
P08	3.72	Sand Fine	Poorly selected	Leptokurtics
P09	4.32	Very Fine Sand	Very Poorly selected	Platykurtics

Only points P01 and P05 showed significant differences in the particle size (ANOVA, $p = 0.05$). There was no significant correlation between the metals in the sediment and the particle size.

The Pejrup diagram shows that most points (P03, P04, P05, P06, P07, and P09) were associated with moderate hydrodynamic conditions. Among them, only P04 and P09 showed a predominance of sand deposited under moderate hydrodynamic conditions (groups B and II). P03, P05, P06, and P07 showed a predominance of fine grains deposited under the same hydrodynamic conditions (Groups C, II, D, and II).

P01 was associated with the predominance of sand deposited under low hydrodynamic conditions (Groups B and I). P02 and P08 were the only ones indicated under high hydrodynamics (groups C and III, and B and III, respectively) (Fig. 2).

Metal concentration in sediments

The concentrations of Zn, Cu, Pb, Cr, Mn, and Fe in the surface sediments at the nine sampled points are summarized in Table 6. Based on the mean values, the concentration pattern followed the order Fe > Mn > Cr > Zn > Cu > Pb at all collection points except for P07, whose pattern followed the order Fe > Mn > Zn > Cr > Cu > Pb.

Table 6 Metal concentrations (μg/g) in the surface sediment of the collection points (mean ± standard deviation). [1]Regional background mean values (De Paula Filho et al. 2015); [2]World average values of

shale metals (Turekian and Wedepohl 1961)

Points	Zn (µg/g)	Cu (µg/g)	Pb (µg/g)	Cr (µg/g)	Mn (µg/g)	Fe (µg/g)
BG[1]	13.40	6.80	5.90	18.00	633.00	14,000.00
Global[2]	95.00	45.00	20.00	90.00	850.00	47,200.00
P01	14.99 ± 9.13	14.29 ± 3.87	4.20 ± 1.49	17.82 ± 12.29	86.84 ± 58.43	15,575.97 ± 10,611.76
P02	32.84 ± 4.09	21.05 ± 2.27	8.78 ± 0.05	40.26 ± 4.56	152.65 ± 42.81	33,507.13 ± 3,391.63
P03	57.09 ± 55.71	16.88 ± 7.38	13.39 ± 2.40	39.77 ± 32.27	233.30 ± 193.82	14,658.37 ± 11,901.80
P04	31.01 ± 5.95	19.91 ± 1.77	9.00 ± 1.33	36.44 ± 6.11	151.86 ± 34.18	28,437.13 ± 4,911.12
P05	14.16 ± 6.47	14.13 ± 3.53	4.50 ± 0.33	18.02 ± 11.14	116.28 ± 64.53	10,953.14 ± 6,962.80
P06	28.98 ± 12.71	17.31 ± 5.80	6.97 ± 3.45	33.76 ± 12.03	153.58 ± 53.00	34,950.35 ± 5,493.24
P07	12.07 ± 6.91	10.10 ± 1.38	2.52 ± 0.00	11.06 ± 6.17	19.53 ± 19.49	12,300.30 ± 4,437.28
P08	23.93 ± 13.74	17.38 ± 4.06	5.97 ± 1.18	26.80 ± 16.06	118.98 ± 60.23	23,323.01 ± 13,289.23
P09	15.17 ± 8.47	13.13 ± 3.78	3.81 ± 0.97	15.73 ± 10.76	70.14 ± 38.50	11,957.34 ± 7,209.23

The concentrations obtained presented a normal distribution and homogeneity of variances only for Fe (Shapiro-Wilk, $p > 0.05$; Levene, $p > 0.05$). Fe was also the only element that showed a significant difference between P05 and P06 (ANOVA, $p < 0.05$). The other metals did not show significant differences between collection points.

The highest concentrations of metals were recorded in the sediments of the SMEC port area, with concentrations exceeding the regional background values (Table 6). The lowest and highest mean values of Zn were recorded in P07 (12.07 + 6.91 µg/g) and P03 (57.09 + 55.71 µg/g), respectively. The furthest point from the port area, P07, recorded the lowest mean values for Cu (10.10 + 1.38 µg/g), Pb (2.52 + 0.00 µg/g), Cr (11.06 + 6.17 µg/g) and Mn (19.53 + 19.49 µg/g). The highest mean values of Cu, Cr, Pb, and Mn were recorded in the port areas, P02 (Cu = 21.05 + 2.27 and Cr = 40.26 + 4.56 µg/g) and P03 (Pb = 13. 39 + 2.40 and Mn = 233.30 + 193.82 µg/g).

All registered values of the sampling points were lower than those of TEL, PEL, ERL, and ERM (Fig. 3). Cu was an exception, as its concentrations were higher than the TEL in P02 (Cu = 21.05) and P04 (Cu =

19.91). All points registered concentrations below those established by the national legislation contained in Resolutions 344/2004 and 454/2012 of the National Council for the Environment (CONAMA, Brazil) for estuarine and marine sediments, whose guidelines are based on ERL and ERM values.

Metal concentration in macroalgae

The concentrations of Zn, Cu, Pb, Cr, Mn, and Fe in the macroalgae between the sampling points are summarized in Table 7.

The highest (48.03 µg/g) and lowest (0.37 µg/g) Zn values were detected in B. radicans rhodophyte at P01 and P09, respectively. The species *R. africanum* and *C. caespitosa* had the highest (10.72 µg/g) and lowest (1.30 µg/g) Cu values, recorded in P03 and P04, respectively.

The highest concentration (5.61 µg/g) of Pb was recorded in P04, and the lowest (1.00 µg/g) in P06 in the macroalgae *C. membranacea*. Cr had the lowest concentration detected in the species *C. caespitosa* (2.06 µg/g) and the highest in the species *R. africanum* (19.90 µg/g), also recorded in P04 and P06, respectively (Table 7).

The concentrations of Mn and Fe were higher in all species than those of the other quantified elements (ANOVA, $p < 0.05$). Mn showed a high variation between the highest (825.86 µg/g) and the lowest (13.56 µg/g) values, detected in *C. membranacea* (P05) and *R. africanum* (P04). Fe also showed a high rate of variation between the highest (8060.56 µg/g) and lowest (2.26 µg/g) values, detected in *C. membranacea* (P04) and *C. caespitosa* (P09) (Table 7).

Table 7 Metal concentration (µg/g) in macroalgae by collection point, in the mangroves of São Luis Island, Maranhão

Bioaccumulation Factor in Macroalgae

Figure 4 shows the bioaccumulation factor (BCF), indicating that almost all macroalgae collected in this study were susceptible to bioaccumulation. *B. radicans* recorded the highest bioaccumulation value for Mn (2.22) and the lowest for Pb (0.31). *C. caespitosa*, also Rhodophyceae, showed low bioaccumulation values compared to the other species (Cu = 0.15, Pb = 0.001, Cr = 0.09, Mn = 0.64, and Fe = 0.03).

C. caespitosa was significantly different from the chlorophytes *C. membranacea* and R. africanum (ANOVA, $p < 0.05$). The BCF for *R. tortuosum* was impossible to calculate because obtained values did not exceed the detection level.

Points	Macroalgae	Zn (µg/g)	Cu (µg/g)	Pb (µg/g)	Cr (µg/g)	Mn (µg/g)	Fe (µg/g)
P01	*B. radicans*	48.03	8.51	2.91	15.64	460.74	4772.68
	C. caespitosa	28.89	1.63	N/D	2.14	64.83	549.02
	C. membranacea	11.64	1.89	2.84	9.60	119.12	3748.82
	R. africanun	36.02	7.56	2.97	19.00	125.17	5501.22
P03	*R. africanun*	38.81	10.72	3.53	18.97	125.86	5653.26
	B. radicans	27.69	8.84	1.73	8.64	286.53	2761.03
	C. membranacea	21.54	8.61	4.28	15.00	272.28	6279.84
P04	*B. radicans*	26.36	6.41	1.49	10.44	162,76	3093.81
	C. caespitosa	12.04	1.30	N/D	2,06	71,23	683.93
	C. membranacea	28.95	8.14	5,61	19.17	299.66	8060.56
	R. africanun	5.18	1.49	1.58	2.81	13.56	7248.34
P05	*C. membranacea*	23.60	8.74	3.38	16.71	825.86	5648.55
P06	*R. africanun*	31.08	8.32	2.27	19.90	109.08	6604.72
	C. membranacea	21.46	6.09	1.00	16.68	467.77	7231.25
	C. caespitosa	16.26	4.82	N/D	3.52	107.41	975.58
	B. radicans	20.15	5,92	1.64	11.08	195.82	3722.59

The pattern of metal bioaccumulation in the macroalgal species was in the following order: *Bostrychia radicans* (Mn > Zn > Cu > Cr > Pb > Fe), *Catenella caespitosa* (Zn > Mn > Cu > Cr > Fe > Pb), *Cladophoropsis membranacea* (Mn > Zn > Cr > Pb > Cu > Fe), and *Rhizoclonium africanum* (Zn > Mn > Cr > Cu > Pb > Fe).

Geo-accumulation index (I_{geo})

The Geoaccumulation index (I_{geo}) was calculated to quantify metal pollution in the sediment, the values of which are shown in Figure 5. In general, the sampled points presented an I_{geo} below two, which characterizes the environment as moderately contaminated to non-contaminated.

The points closest to the port areas (P01, P02, P03, and P04) showed moderate contamination (I_{geo} = 0 – 1) of two or more metals. The highest Igeo values were identified in P03 and P07 for Zn (I_{geo} = 1.51) and Cu (I_{geo} = 1.05). However, Mn was below 0 at all collection points, characterizing them as non-contaminated for this element. Although the I_{geo} values varied between environments, only Fe showed a significant difference (ANOVA, $p < 0.05$) between points P05 and P06 (Fig. 5).

As for CF, only Mn showed values below one at all sampled points, indicating low contamination of this metal in mangroves. In general, based on the CF values, the environment tended to be moderately contaminated. P02 and P03 exhibited considerable contamination with Cu (CF = 3.10) and Zn (CF = 4.26), respectively. The other elements followed the general trend of moderate contamination. P02, P03, P04, and P06 recorded PLI values above 1, indicating contamination in these environments. The other points had PLI values below 1, indicating zero contamination (Fig. 6).

PLI and CF did not show significant differences between the collection points (ANOVA, $p > 0.05$; Kruskal-Wallis, $p > 0.05$).

To assess the contribution of natural and anthropogenic sources to mineral enrichment at the collection points, an enrichment factor was applied, as summarized in Figure 7. In general, the environment showed a tendency towards minimal mineral enrichment ($1 < EF < 3$). Zn and Cu presented EF values above five at P03, indicating significant enrichment at this point. The EF values for Cu at all collection points, except P03 and P05, were between 1.5 and 3 (minimum enrichment), showing anthropogenic influence for this metal. P03 was statistically different at all points for all metals (Kruskal-Wallis, $p < 0.05$).

Discussion

The values of physical and chemical variables obtained in this study agree with those recorded for both SMEC and SJEC by Cavalcanti and Cutrim (2018) and Serejo et al. (2020).

Although many studies point to salinity, pH, and DO variables as relevant to the mobility of metals in estuarine environments (Karbassi et al. 2014; Karbasi and Heidari 2015; Li et al. 2013; Samani et al. 2014), these parameters showed weak positive correlations, although not significant, with the metal values in the sediments. However, among the parameters measured in this study, temperature was moderately to strongly related to Zn ($r = 0.686$, $p = 0.041$), Pb ($r = 0.751$, $p = 0.020$), and Cr ($r = 0.764$, $p = 0.017$) in the sedimentary compartment. This highlights sediment as a potential source of these metals for interstitial and surrounding waters.

It is known that high temperatures provide a high release of metals from the sediment to the liquid medium, which, consequently, are bioavailable for macroalgae (Li et al. 2013; Schuhmacher et al. 1995; Zhao et al. 2013), because such organisms only accumulate metallic ions dissolved in water (Luoma 1983; Luoma et al. 1982).

Only OD showed a significant correlation with metal concentrations in macroalgae. Such correlations were observed between the OD and Cu ($r = 0.675$; $p < 0.05$), Cr ($r = 0.694$; $p < 0.05$), and Mn ($r = 0.716$; $p < 0.05$). This is the same relationship reported by Macedo et al. (2009), who found that the copper content in rhodophyte species is influenced by dissolved oxygen. Studies that address the relationship between the accumulation of metals in macroalgae and OD are scarce, thus compromising our understanding of this interaction.

Some studies have described the influence of DO on metals adsorbed to the sediment (Atkinson et al. 2007; Huang et al., 2017; Kang et al. 2019; Li et al. 2013; Liu et al. 2019). OD values ranging between 7.0 and 9.0 mg/L promote the release of metals from the sediment to the interstitial water (Li et al. 2013), becoming bioavailable for macroalgae, while OD values lower than 7.0 mg/L provide little or no release of metals to water, depending on the metal (Li et al. 2013).

Conversely, OD values lower than 7.0 mg/L provide little or no release of metals to water, depending on the metal (Li et al. 2013); this primarily occurs if such values are observed due to the intense degradation of organic matter (Gerringa 1991), which may explain the high concentrations of metals in P09. At the time of collection, domestic sewage was discharged directly into the sampling location at P09.

Metals in sediment

The metal concentrations obtained in the sediment samples were compared with the world mean concentrations of metals in shale (Turekian and Wedepohl 1961) and the regional average (De Paula Filho et al. 2015) (Table 6). Regarding the global average, the results of this study were well below; however, above the regional average, sometimes on the order of two to three times higher. Mn was the exception, being below global and regional concentrations, corroborating the assertion of non-contamination of the environment by this metal (Table 6).

The global values proposed by Turekian and Wedepohl (1961) are high and therefore may not be representative of different sedimentary basins. Thus, it is necessary to define the use of background values at local or regional levels, according to the content deposited in the sedimentary basin in pre-industrial times (De Paula Filho et al. 2015; De Paula Filho et al. 2021).

Only Fe showed a significant difference among the sampling points (ANOVA, $p > 0.05$). However, all metals were significantly strongly and positively correlated with each other, indicating common sources and processes (De Paula Filho et al. 2021). Zn ($r = 0.917$; $p < 0.01$), Pb ($r = 0.950$; $p < 0.01$), and Cr ($r = 0.894$; $p < 0.01$) were strongly correlated with Mn, indicating the probable adsorption of these metals to Mn oxide hydroxides (Chakraborty et al. 2014; Udechukwu et al. 2014). In contrast, Cu ($r = 0.808$; $p < 0.01$) was more strongly correlated with Fe, indicating the probable adsorption of Cu to Fe oxide hydroxides (Chakraborty et al. 2014).

Mn manifested itself as a metal carrier for the sediment in the estuarine complexes of the Brazilian equatorial margin, probably because of its high oxidation resistance and subsequent flocculation, remaining longer in the water column and thus adsorbing a greater number of metals onto Fe. Mn tends to deposit in the form of oxyhydroxide only when oxygen-rich marine waters enter the estuary (Lacerda et al. 1999).

Santos et al. (2019) verified that significant differences were observed between Mn, Fe, and Zn in SMEC, suggesting different origins and carriers, and Fe and Mn showed strong correlations with each other.

Such results are contrary to those of this study, which suggests the relevant capacity of the system to behave in different ways depending on the level of contamination to which it is exposed. However, both studies point to similar behaviors for Cu, Pb, and Cr.

Geochemical indices

Geochemical indices are essential for analyzing contamination at sampling points. Although metals have been shown to have values higher than the regional background at some points, only the indices showed specific information regarding the degree of contamination. In general, the indices indicated moderate contamination of the studied environments.

Igeo ranged between 0 and 2, particularly at points associated with the adjacencies of port areas. P02, P03, P04, and P06 recorded ICP values above 1, indicating contamination in these environments. FC indicated that P02 and P03 were considerably contaminated with Cu (FC = 3.10) and Zn (FC = 4.26), respectively. As for mineral enrichment, only P02 and P06 did not show an anthropogenic influence on metal concentrations (FE < 1.5). P03 showed significant enrichment for Zn and Cu.

Several studies have evaluated metal contamination in port areas worldwide, highlighting these areas as potential sources of Zn, Cu, Cr, and Pb (Buruaem et al. 2012; Hortellani and Sarkis 2008; Jahan and Strezov 2019; Sari et al. 2014; Shafie et al. 2012). The results for the port area of the Brazilian equatorial margin were not different because, in general, the indices showed Zn, Cu, and Cr as the principal contaminants of the sampled environments, originating from anthropogenic sources, particularly Cu.

In port areas, metals such as Pb and Cr can originate from erosion of ship hulls. In turn, Cu can be released by the antifouling paint used on boats and ships (Santos et al. 2019; Shafie et al. 2012).

The strong positive and significant correlations between all sampled points ($r > 0.9$; $p < 0.01$) suggest that the estuarine complexes of Maranhão, CESM and CESJ, share similar sources and processes responsible for controlling the mobility and bioavailability of metallic elements. However, although there are similarities, the points located in the CESM seem to suffer from high interference in terms of sources and processes. For example, P02, P03, and P04 exceeded two to three times the regional background values (Table 6), demonstrating relevant levels of contamination, as evidenced by the different geochemical indices. The gradient of metal concentrations observed from P01 to P05 must be associated with the local hydrodynamics, which should trap metals in this region.

Local hydrodynamics seem to contribute to the imprisonment of metals between these points, as there was a gradient in metal concentrations from P01 to P05. Points P02, P03, and P04 are in places with low depth (< 20 m) and currents with speeds of less than 1.1 m/s (González-Gorbeña et al. 2015), which can favor flocculation and deposition processes at such points. In SMEC, high concentrations of metals in low-energy zones have already been reported by Santos et al. (2019), who pointed out that in these zones, metals have more binding capacity to fine sediments and organic material, furthering the flocculation

process. This effect was evident when comparing the metal concentrations in the sediment and the results of the Pejrup diagram. P02, P03, and P04 presented low-to-moderate hydrodynamics and the highest concentrations of metals in the sediment (Fig. 2; Table 6).

TEL, PEL, ERL, and ERM

Compared with the TEL, PEL, ERL, and ERM values, the metal concentrations between the points were well below the established limits, except for the Cu concentrations in P02 and P04, which were above the TEL and below the PEL (Fig. 3).

This range between the TEL and PEL draws attention to possible adverse effects on the biological community (Hortellani et al. 2008; De Paula Filho et al. 2021). Therefore, although Cu is an essential element, it can be toxic to aquatic organisms, especially those that live or are in direct contact with sediment when their values are within this range (CCME 1999).

In Brazil, ERL and ERM limits were adopted as reference values by Resolutions 344/2004 and 454/2012 of the National Council for the Environment (CONAMA, Brazil) for estuarine and marine sediments. Therefore, the sampled points comply with national legislation.

De Paula Filho et al. (2021) observed this Cu performance in the Parnaíba Delta, a region located on the Brazilian equatorial margin, whose concentrations exceeded the TEL at 61% of the sampling sites, mainly in areas with more sediment deposition.

Metals in macroalgae

The macroalgae recorded at the sampling points are typical of Brazilian mangrove areas (Fernandes and Alves 2011; Oliveira-Filho 1984; Yokoya et al. 1999).

The lack of rocky substrate, low salinity, and high turbidity of coastal waters make the island of São Luís an environment with low diversity of macroalgae (Oliveira-Filho 1984). These conditions favor the dominance of species adapted to mangrove ecosystems. Macroalgal species grow epiphytically in pneumatophores, rhizophores, and trunks (Phillips et al. 1994; Phillips et al. 1996), as is the case with the species found in this study.

The correlation values between the concentrations of metals in macroalgae and sediments ranged from 0.829 to 1 ($p < 0.05$), which showed strong significant correlations and demonstrated that macroalgal bioaccumulation is strongly associated with the concentrations of metals found in sediments.

Bioaccumulation factor (BCF)

All macroalgae bioaccumulate in different orders and magnitudes according to their BCF. Although macroalgae share the same habitat and conditions, they exhibit particularities in metal accumulation, such as life span, morphology, contact surface area, growth rate, and selective metal affinities (Chakraborty et al. 2014; Schintu et al. 2010). Among the essential metals, absorption followed the order Mn > Zn > Cu > Fe for *B. radicans* and *C. membranacea*, whereas *C. caespitosa* and *R. africanum* followed the order Zn > Mn > Cu > Fe.

Among the non-essential metals, the absorption process followed the order of Cr > Pb for both groups of macroalgae. Chlorophyceae biosorbed Cr and Pb (non-essential) at higher concentrations than essential metals, such as Cu and Fe.

The biosorption process occurs in macroalgae because cell wall polysaccharides have functional groups (hydroxyl, sulfate, and carboxyl) that act as ion exchangers and bind to metallic cations. (Trifan et al. 2015). Once adsorbed to the cell wall, metals can precipitate through the excretion of metabolic products by macroalgae or be transported slowly into the cytoplasm through chemisorption (Veglio and Beolchini 1997). This last process is the most harmful, as metals reaching the cytoplasm and bioaccumulation can cause adverse effects on macroalgae, such as oxidative stress, inhibited photosynthesis and chlorophyll production, and deficient macroalgal growth (Baumann et al. 2009; Gledhill et al. 1997; Pinto et al. 2003).

The bioaccumulation of metals is not restricted to microalgae as primary producers because, once absorbed, these metals can be transferred along the food chain and reach humans (Santos et al. 2019).

Thick macroalgae tend to have lower metal concentrations than filamentous macroalgae (Trifan et al. 2015), which explains the reduced accumulation values in *C. caespitosa* compared to other species. Chlorophyceous showed a better accumulation response at the sampled points, with high observed concentrations of metals, most of which were non-essential metals. This affinity of chlorophytes with metals can be attributed to their growth in direct contact with the sediment and the surrounding water, especially *C. membranacea*, which adheres to the muddy substrate and retains large amounts of sediment owing to its cushion-like morphology.

The results obtained in this study are similar to those of other studies conducted on other mangroves. Chlorophytes are excellent biomonitors owing to their high capacity to reflect environmental contamination. Chakraborty et al. (2014) verified the efficiency of *Ulva lactuca* in accumulating high levels of Cu, Fe, and Zn, and Akcali and Kucuksezgin (2011) reported high levels of Cu, Pb, Zn, and Fe.

During the absorption process, macroalgae tend to control the composition and concentration of essential metals when they are available in the environment at levels that only satisfy the needs of metabolism and growth. When these levels exceed those required by the organism, biological regulation is impaired owing to external forcing. Consequently, macroalgae accumulate high levels of essential metals and concomitantly accumulate these non-essential metals (Baoli and Congqiang 2004). The

strong positive and significant correlations between metal concentrations in macroalgae and sediment, accompanied by the high values recorded for the bioaccumulation factor, reinforce this statement.

Mn is an essential metal required by macroalgae, and in this study, it was a relevant carrier of metals such as Zn, Pb, and Cr to the sediment. Mn was the most bioaccumulated metal (Table 9), and we realized that it influenced the bioaccumulation of these metals. Hall and Brown (2002) demonstrated that the association between Mn and Cu results in a high absorption of Cd in macroalgae.

The representativeness of *C. membranacea* in the bioaccumulation of Mn in relation to other species allows it to be chosen as a key species for monitoring this metal and others associated with it. Compared to Chlorophyceae, the two species of Rhodophyceae proved to be better biomonitors for assessing environmental contamination by Fe (Kruskal-Wallis; $p < 0.05$). Therefore, the use of the four species of macroalgae is complementary and essential for a broader response to contaminants in mangrove ecosystems.

Conclusion

The metal concentrations recorded in the sediments of both estuarine complexes were below the mean values of the global background but above the regional level. This reinforces what past studies have pointed out regarding the need to carry out local and regional surveys of the concentrations of metals deposited in pre-industrial times, as the high global mean values may not be representative of the different sedimentary basins.

The geochemical indices indicate moderate contamination and enrichment among the studied environments, showing significant enrichment of Zn and Cu in the regions under the influence of port activity. This result reinforces the idea that, although there is contamination by metals in other estuarine areas on the Brazilian equatorial margin, port activity remains a relevant source of contaminants in the estuarine environment.

Local hydrodynamics have a significant influence on the metal deposition process in areas close to harbor regions. Cu concentrations were above the TEL and below the PEL, indicating possible adverse effects on the biological community. The results showed different relationships from those reported in previous studies, indicating different environmental responses to their exposure to contaminants.

The absence of significant differences and strong correlations between metals suggests similar sources and processes for the deposition of these elements in the equatorial margin of Brazil. Mn showed a strong positive correlation with Zn, Pb, and Cr, which proved to be excellent metal carriers in this region.

All macroalgae bioaccumulate metals, demonstrating the biomonitor potential of these organisms. The species showed different patterns of bioaccumulation; however, Mn and Zn were the most bioaccumulated. The divergent behavior in the bioaccumulation pattern among macroalgae suggests

that monitoring different species is essential for a more accurate response to environmental contamination by different types of metals.

We suggest complementary studies to verify possible seasonal variations in the bioaccumulation patterns of macroalgae associated with mangroves on the Brazilian equatorial margin, primarily because the dynamics of metal bioaccumulation in the macroalgal species found in this area are poorly investigated in the international scene, this being the main difficulty of this work. In this way, we bring preliminary information about the accumulation of metals regarding the species found in our investigation.

Statements And Declarations

Funding

The authors declare that no funds, grants, or other support were received during the preparation of this manuscript.

Consent for publication

Not applicable

Competing Interests

The authors have no relevant financial or non-financial interests to disclose.

Author Contributions

All authors contributed to the study conception and design. JC: Conceptualization, methodology, data collection, analysis, writing-original draft and editing. MC: Conceptualization, methodology, writing-original draft, writing-review and editing, and supervision.

Ethical Approval and consent to participate

Not applicable

Availability of data and materials

The authors certify that all data and materials, as well as the software application or custom code, support their published claims and meet field standards.

Acknowledgments

This research was supported by grand given by Foundation for Research and Scientific and Technological Development of Maranhão – Brazil (FAPEMA) through the concession of a Master's scholarship (BM-00061/20) to the first author. The authors would like to thank the Postgraduate Program

in Oceanography (PPGOceano- UFMA) as well as the Laboratory of Phytoplankton of Federal University of Maranhão (UFMA) and Laboratory of Environmental Science (UENF) for technical and structural support.

References

1. Akcali I, Kucuksezgin F (2011) A biomonitoring study: Heavy metals in macroalgae from eastern Aegean coastal areas. Mar Pollut Bull 62(3):637-645
2. Amado Filho GM, Andrade LR, Karez CS, Farina M, Pfeiffer WC (1999) Brown algae species as biomonitors of Zn and Cd at Sepetiba Bay, Rio de Janeiro, Brazil. Mar Environ Res 48(3):213-224
3. Atkinson CA, Jolley DF, Simpson SL (2007) Effect of overlying water pH, dissolved oxygen, salinity and sediment disturbances on metal release and sequestration from metal contaminated marine sediments. Chemosphere 69:1428–1437
4. Baoli W, Congqiang L (2004) Factors controlling the distribution of trace metals in macroalgae. Chin J Geochem 23(4):366-372
5. Baumann HA, Morrison L, Stengel DB (2009) Metal accumulation and toxicity measured by PAM—Chlorophyll fluorescence in seven species of marine macroalgae. Ecotox Environ Safe 72(4):1063-1075
6. Billah MM, Kamal, AHM, Idris MH, Ismail J (2017) Mangrove Macroalgae as Biomonitors of Heavy Metal Contamination in a Tropical Estuary, Malaysia. Water Air Soil Pollut 228(9):228-347
7. Brito GB, De Souza TL, Bressy FC, Moura CWN, Korn MGA (2012) Levels and spatial distribution of trace elements in macroalgae species from the Todos os Santos Bay, Bahia, Brazil. Mar Poll Bull 64(10):2238-2244
8. Buruaem LM, Hortellani MA, Sarkis JE, Costa-Lotufo LV, Abessa DMS (2012) Contamination of port zone sediments by metals from Large Marine Ecosystems of Brazil. Marine Pollution Bulletin 64(3):479-488
9. Cavalcanti LF, Cutrim MVJ (2018) Structure of microphytoplankton community and environmental variables in a macrotidal estuarine complex, São Marcos Bay, Maranhão – Brazil. Braz J Ocean 66(3):283-300
10. CCME (1999) Canadian Sediment Quality Guidelines for the Protection of Aquatic Life – Copper. Canadian Environmental Quality Guidelines, Canadian Council of Ministers of the Environment
11. Chakraborty S, Bhattacharya T, Singh G, Maity JP (2014) Benthic macroalgae as biological indicators of heavy metal pollution in the marine environments: A biomonitoring approach for pollution assessment. Ecotox Environ Safety 100:61-68
12. Climate-Data (2021) São Luís Clima. https://ptclimate-dataorg/america-do-sul/brasil/maranhao/sao-luis-1671/. Acessed 20 January 2021 (in portuguese)
13. Conti ME, Cecchetti GA (2003) Biomonitoring study: trace metals in algae and molluscs from Tyrrhenian coastal areas. Environ Res 93:99-112

14. CPRM (2000) Programa Levantamentos Geológicos Básicos do Brasil - São Luís NE/SE, Folhas SA23-X e SA23-Z Estados do Maranhão e Piauí Brasília (in portuguese)
15. Dawes C, Siar K, Marlett, D (1999) Mangrove structure, litter and macroalgal productivity in a northern-most forest of Florida. Mangrov Salt Mars 3:259-267
16. De Paula Filho FJ et al (2021) Assessment of heavy metals in sediments of the Parnaíba River Delta in the semi-arid coast of Brazil. Environ Earth Sci 80:167
17. De Paula Filho FJ et al (2015) Background values for evaluation of heavy metal contamination in sediments in the Parnaíba River Delta estuary, NE/Brazil. Mar Pollut Bull 91(2):424–428
18. Diniz C, Cortinhas L, Nerino G, Rodrigues J, Sadeck L, Adami M, Souza-Filho PWM (2019) Brazilian Mangrove Status: Three Decades of Satellite Data Analysis. Remote Sens 11(808):2-19
19. Fernandes MEB, Alves EFS (2011) Occurrence and distribuition of macroalgae (Rhodophyta) associated with mangroves on the Ajuruteua Peninsula, Bragança, Pará, Brasil. UAKARI 7(2):35-42
20. Ferreira AC, Lacerda LD (2016) Degradation and conservation of Brazilian mangroves, status and perspectives. Oc Coast Manag 125:38-46
21. Folk RL, Ward WC (1957) A Study in the Significance of Grain-Size Parameters. J Sedim Petrol 27:3-26
22. Gerringa L (1991) Mobility of Cu, Cd, Ni, Pb, Zn, Fe and Mn in marine sediment slurries under anaerobic conditions and at 20% air saturation. Neth J Sea Res 27(2):145–156
23. Gledhill M, Nimmo M, Hill SJ, Brown MT (1997) The toxicity of copper (II) species to marine algae, with particular reference to macroalgae. J Phycol 33(1):2-11
24. González-Gorbeña E, Rosman PCC, Qassim RY (2015) Assessment of the tidal current energy resource in São Marcos Bay, Brazil. J Ocean Eng Mar Energy 1(4):421–433
25. Gruber NLS, Barboza EG, Nicolodi JL (2003) Geografia dos sistemas costeiros e oceanográficos: Subsídios para gestão integrada da zona costeira. Gravel 1(1):81-89 (in portuguese)
26. Hakanson L (1980) An ecological risk index for aquatic pollution control: a sedimentological approach. Water Res 14(8):975-1001
27. Hall MJ, Brown MT (2002) Copper and Manganese influence the uptake of cadmium in marine macroalgae. Bull Environ Contamin Toxicol 68(1):49–55
28. Hortellani MA, Sarkis JES, Abessa DMS, Sousa ECPM (2008) Avaliação da contaminação por elementos metálicos dos sedimentos do Estuário Santos – São Vicente. Quim Nova 31(1):10-19
29. Huang Y, Zhang D, Xu Z, Yuan S, Li Y, Wang L (2017) Effect of overlying water pH, dissolved oxygen and temperature on heavy metal release from river sediments under laboratory conditions. Arch Environ Prot 43:28-36
30. Jahan S, Strezov V (2019) Assessment of trace elements pollution in the sea ports of New South Wales (NSW), Australia using oysters as bioindicators. Sci Report 9:1416
31. Jha B, Reddy CRK, Thakur MC, Rao UM (2009) Seaweeds of India: The diversity and distribution of seaweeds of the Gujarat coast. Springer, Dordrecht

32. Kang M, Tian Y, Peng S, Wang M (2019) Effect of dissolved oxygen and nutrient levels on heavy metal contents and fractions in river surface sediments. Sci Total Environ 648:861–870
33. Karbassi AR, Heidari M (2015) An investigation on role of salinity, pH and DO on heavy metals elimination throughout estuarial mixture. Glob J Environ Sci Manag 1(1):41-46
34. Karbassi AR et al (2014) Dissolved and particulate trace metal geochemistry during mixing of Karganrud River with Caspian Sea water. Arab J Geosci 8(4):2143–2151
35. Karez CS, Magalhaes VF, Pfeiffer WC, Amado Filho GM (1994) Trace metal accumulation by algae in Sepetiba Bay, Brazil. Environ Poll 83(3):351-356
36. Lacerda LD, Ribeiro J, Gueiros BB (1999) Manganese dynamics in a mangrove mud flat tidal creek in SE Brazil. Mang Salt Marsh 3(2):105–115
37. Lacerda LD, Teixeira VL, Guimarães JRD (1985) Seasonal Variation of Heavy Metals in Seaweeds from Conceição de Jacareí (RJ), Brazil. Bot Mar 28(8)
38. Li H, Shi A, Li M, Zhang X (2013) Effect of pH, Temperature, Dissolved Oxygen, and Flow Rate of Overlying Water on Heavy Metals Release from Storm Sewer Sediments. J Chem 2013:1–11
39. Liu JJ, Diao ZH, Xu XR, Xie Q (2019) Effects of dissolved oxygen, salinity, nitrogen and phosphorus on the release of heavy metals from coastal sediments. Sci Total Environ 666:894-901
40. Lombardi AT, Vieira AAH (1998) Copper and lead complexation by high molecular weight compounds produced by Synura sp (Chrysophyceae). Phycol 37:34-39
41. Long ER, Macdonald DD, Smith SL, Calder FD (1995) Incidence of adverse biological effects within ranges of chemical concentrations in marine and estuarine sediments. Environ Manag 19(1):81-97
42. Luoma SN (1983) Bioavailability of trace metals to aquatic organisms – a review. Sci Total Environ 28:1–22
43. Luoma SN, Bryan GW, Langstone WT (1982) Scavenging heavy metals from particles by brown seaweed. Mar Poll Bull 13:394–396
44. Macedo SJ, Calado SCS, Koening ML, Silva VL, Neumann-Leitão S (2009) Concentrations of heavy metals in macroalgae in the tropical western Atlantic. Water Res Manag V 125:209-218
45. Machado ALS, Ferreira AG, Zalmon IR (2003) Metais em macroalgas marinhas na costa norte do estado do Rio de Janeiro, Brasil. Trop Ocean 31(1):71-80 (in portuguese)
46. Mamboya FA, Pratap HB, Mtolera M, Bjork M (1999) The effect of copper on the daily growth rate and photosynthetic efficiency of the brown macroalga *Padina boergensenii*. In: Richmond MD, Francis J (Eds) Proceedings of the Conference on Advances on Marine Sciences in Tanzania, pp 185-192
47. MARCOVECCHIO JE (2000) Overview on land-based sources and activities affecting the marine, coastal and associated freshwater environment in the Upper Southwest Atlantic Ocean. UNEP Regional Seas Reports and Studies No 170, UNEP/GPA coordination Office, The Hague.
48. Marins RV, Freire GSS, Maia LP, Lima JPR, Lacerda LD (2002) Impacts of land-based activities on the Ceará coast, NE Brazil. In: Lacerda LD, Kremer HH, Kjerfve B, Salomons W, Marshall-Crossland JI,

Crossland JC (eds) South American Basins: LOICZ Global Change Assessment and Synthesis of River Catchment – Coastal Sea Interaction and Human Dimensions LOICZ Reports e Studies No 21, pp 92-98

49. Melville F, Pulkownik A (2007) Investigation of mangrove macroalgae as biomonitors of estuarine metal contamination. Sci Total Environ 387(1-3):301-309
50. MTPA (2018) Plano Mestre Complexo Portuário do Itaqui. Ministério dos Transportes, Portos e Aviação Civil (in portuguese)
51. Muller G (1979) Schwermetalle in den sediment des Rheins: Veranderungem Seit 1971. Umschau 79:778–783
52. Neumann B, Vafeidis AT, Zimmermann J, Nicholls RJ (2015) Future Coastal Population Growth and Exposure to Sea-Level Rise and Coastal Flooding - A Global Assessment. Plos One 10(3)
53. Nittrouer CA, Brunskill GL, Figueiredo AG (1995) Importance of Tropical Coastal Environments. Geo-Mar Lett 15:121-126
54. Nowrouzi M, Pourkhabbaz A (2014) Application of geoaccumulation index and enrichment factor for assessing metal contamination in the sediments of Hara Biosphere Reserve, Iran. Chem Speciat Bioavailab 26:99-105
55. Oliveira-Filho EC (1984) Brazilian mangal vegetation with special emphasis on the seaweeds. In: Por FD, Dor I (Eds) Hydrobiology of the Mangal. Dr W Junk Publishers, Boston
56. Ospina-Álvarez N, Peña EJ, Benítez R (2006) Efecto de la salinidad en la capacidad de bioacumulación de plomo en el alga verde Rhizoclonium riparium (Roth) harvey (Chlorophyceae, Cladophorales). Actual Biol 28(84):17-25
57. Ozkan EY (2012) A new assessment of heavy metal contaminations in an Eutrophicated Bay (Inner Izmir Bay, Turkey) Turk J Fish Aquat Sci 12:135-147
58. Phillips A, Lambert G, Granger JE, Steinke TD (1994) Horizontal zonation of epiphytic algae associated with *Avicennia marina* (Forsk) Vierh pneumatophores at Beach woods mangroves nature reserve, Durban, South Africa. Bot Mar 37:567-576
59. Phillips A, Lambert G, Granger JE, Steinke TD (1996) Vertical zonation of epiphytic algae associated with *Avicennia marina* (Forssk) Vierh pneumatophore at Beachwood Mangrove Nature Reserve, Durban, South Africa. Bot Mar 39:167-175
60. Rebelo-Mochel F (1997) Mangroves on São Luís Island, Maranhão, Brazil In: Kjerfve B, Lacerda LD, Diop EHS (Ed) Mangrove ecosystem studies in Latin America and Africa UNESCO, Paris, pp 145-154
61. Reimann C, De Caritat P (2000) Intrinsic flaws of element enrichment factors (EFs) in environmental geochemistry. Environ Sci Technol 34:5084-5091
62. Reis PA et al (2016) Seaweed *Alaria esculenta* as a biomonitor species of metal contamination in Aughinish Bay (Ireland). Ecol Indic 69:19-25
63. Samani ARV et al (2014) Effect of dissolved organic carbon and salinity on flocculation process of heavy metals during mixing of the Navrud River water with Caspian Seawater. Desalination Water

Treat 55(4):926–934

64. Santos TTL, Marins RV, Da Silva Dias FJ (2019) Carbon influence on metal distribution in sediment of Amazonian macrotidal estuaries of northeastern Brazil. Environ Monitor Assess 191:552
65. Schaeffer-Novelli Y (1995) Manguezal: Ecossistema entre a terra e o mar. Caribbean Ecological Research, São Paulo (in portuguese)
66. Schintu M et al (2010) Macroalgae and DGT as indicators of available trace metals in marine coastal waters near a lead–zinc smelter. Environ Monit Assess 167:653–661
67. Schuhmacher M, Domingo JL, Llobet JM, Corbella J (1995) Variations of heavy metals in water, sediments, and biota from the delta of Ebro River, Spain. J Environ Sci Health Part A 30(6):1361–1372
68. Serejo JHF et al (2020) Fortnightly variability of total suspended solids and bottom sediments in a macrotidal estuarine complex on the Brazilian northern coast. J Sedim Environ 5:101-115
69. Shafie NA, Aris AZ, Zakaria MP, Haris H, Lim WY, Isa NM (2013) Application of geoaccumulation index and enrichment factors on the assessment of heavy metal pollution in the sediments. J Environ Sci Healt Part A 48(2):182–190
70. SILVA RM (2011) Técnica de interferometria SAR e modelagem hidrodinâmica para avaliação de locais adequados ao aproveitamento da energia das correntes de maré. PhD Thesis, Ocean Eng Dep, COPPE—Universidade Federal do Rio de Janeiro
71. Sutherland RA (2000) Bed sediment-associated trace metals in an urban stream, Oahu, Hawaii. Environ Geol 39:611-637
72. Taylor AM, Edge KJ, Ubrihien RP, Maher WA (2017) The freshwater bivalve Corbicula australis as a sentinel species for metal toxicity assessment: an *in situ* case study integrating chemical and biomarker analyses. Environ Toxicol Chem 36:709–719
73. Taylor SR (1964) Abundance of chemical elements in the continental crust: a new table. Geochim Cosmochim Acta 8 (1):1273–1285
74. Trifan A et al (2015) Heavy metal content in macroalgae from Roumanian Black Sea. Rev Roum Chim 60(9):915-920
75. Turekian KK, Wedepohl KH (1961) Distribution of the elements in some major units of the earth's crust. Geol Soc Am Bull 72:175–192
76. Udechukwu BE, Ismail A, Zulkifli SZ, Omar H (2014) Distribution, mobility, and pollution assessment of Cd, Cu, Ni, Pb, Zn, and Fe in intertidal surface sediments of Sg Puloh mangrove estuary, Malaysia. Environ Sci Pollut Res 22:4242–4255
77. Varol M (2011) Assessment of heavy metal contamination in sediments of the Tigris River (Turkey) using pollution indices and multivariate statistical techniques. J Hazard Mater 195:355–364
78. Veglio F, Beolchini F (1997) Removal of Metals by Biosorption: A Review. Hidrometal 44:301-316
79. Wentworth CKA (1992) Scale of grade and class terms for clastic sediments. J Geol 30:377-392

80. Yahya AN, Mohamed SK, Mohamed AG (2018) Environmental Pollution by Heavy Metals in the Aquatic Ecosystems of Egypt. Open Acc J of Toxicol 3(1):001-009
81. Yokoya NS et al (1999) Temporal and spatial variations in the structure of macroalgal communities associated with mangrove trees of Ilha do Cardoso, São Paulo state, Brazil. Braz J Bot 22(2):195-204
82. Zhao S, Shi X, Li C, Zhang H, Wu Y (2013) Seasonal variation of heavy metals in sediment of Lake Ulansuhai, China. Chem Ecol 30(1):1–14
83. Zhiyuan W, Wang D, Zhou H, Qi Z (2011) Assessment of soil heavy metal pollution with principal component analysis and Geoaccumulation Index. Proced Environ Sci 10:1946-1952

Figures

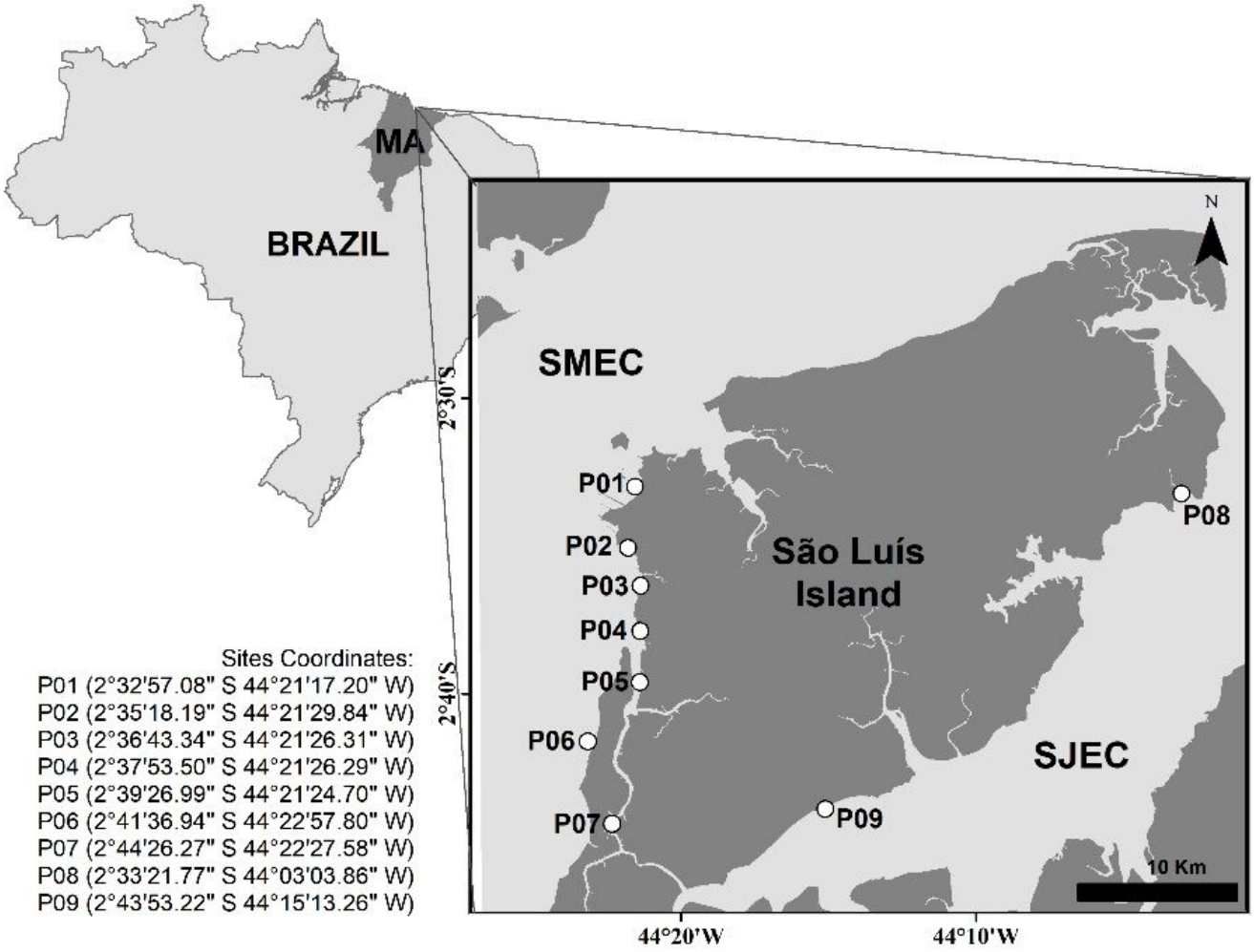

Figure 1

Study area referring to the island of São Luís, Maranhão, Brazil. SMEC- São Marcos Estuarine Complex and SJEC- São José Estuarine Complex

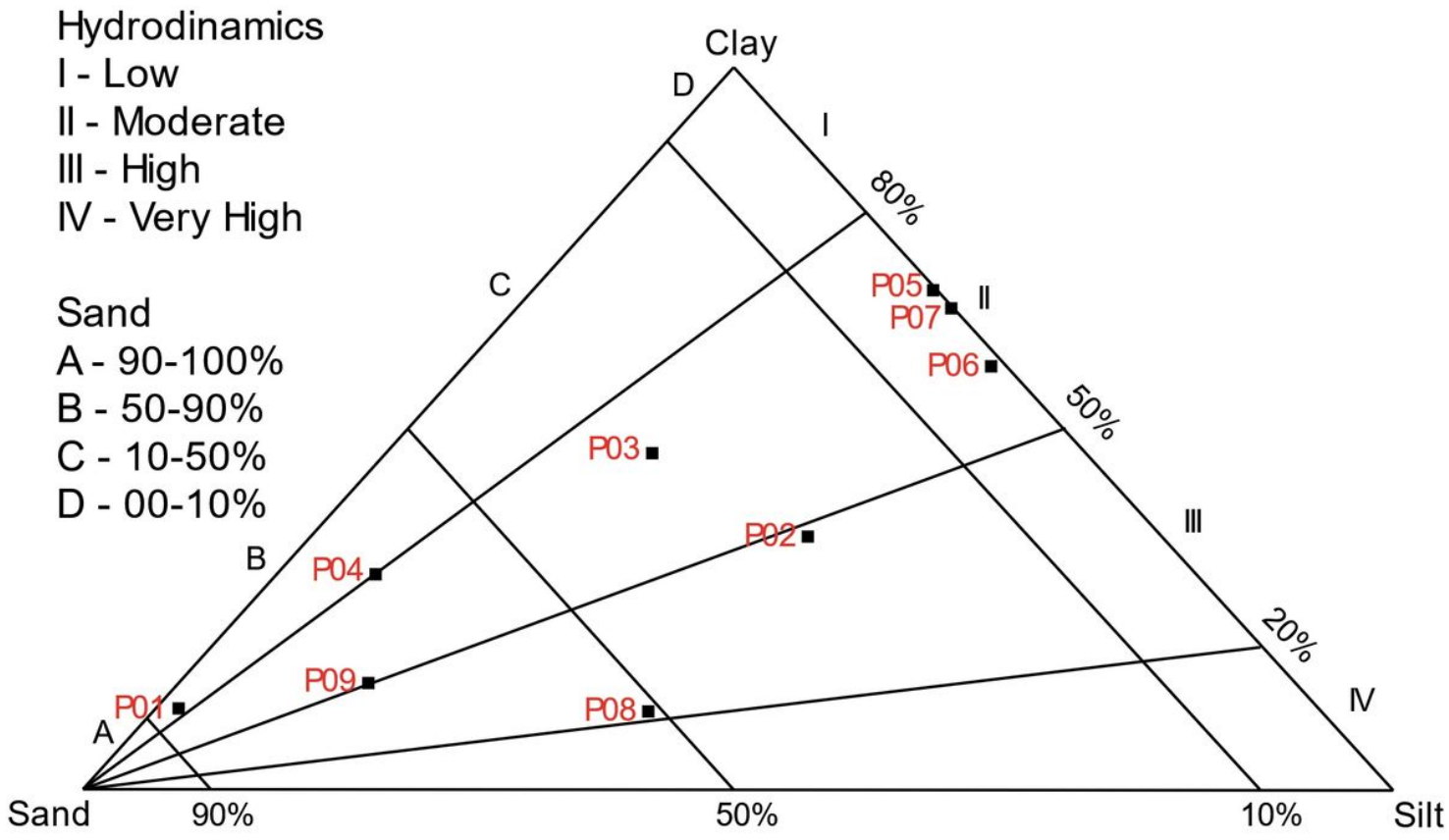

Figure 2

Pejrup diagram (1988) according to particle size analysis of collection points

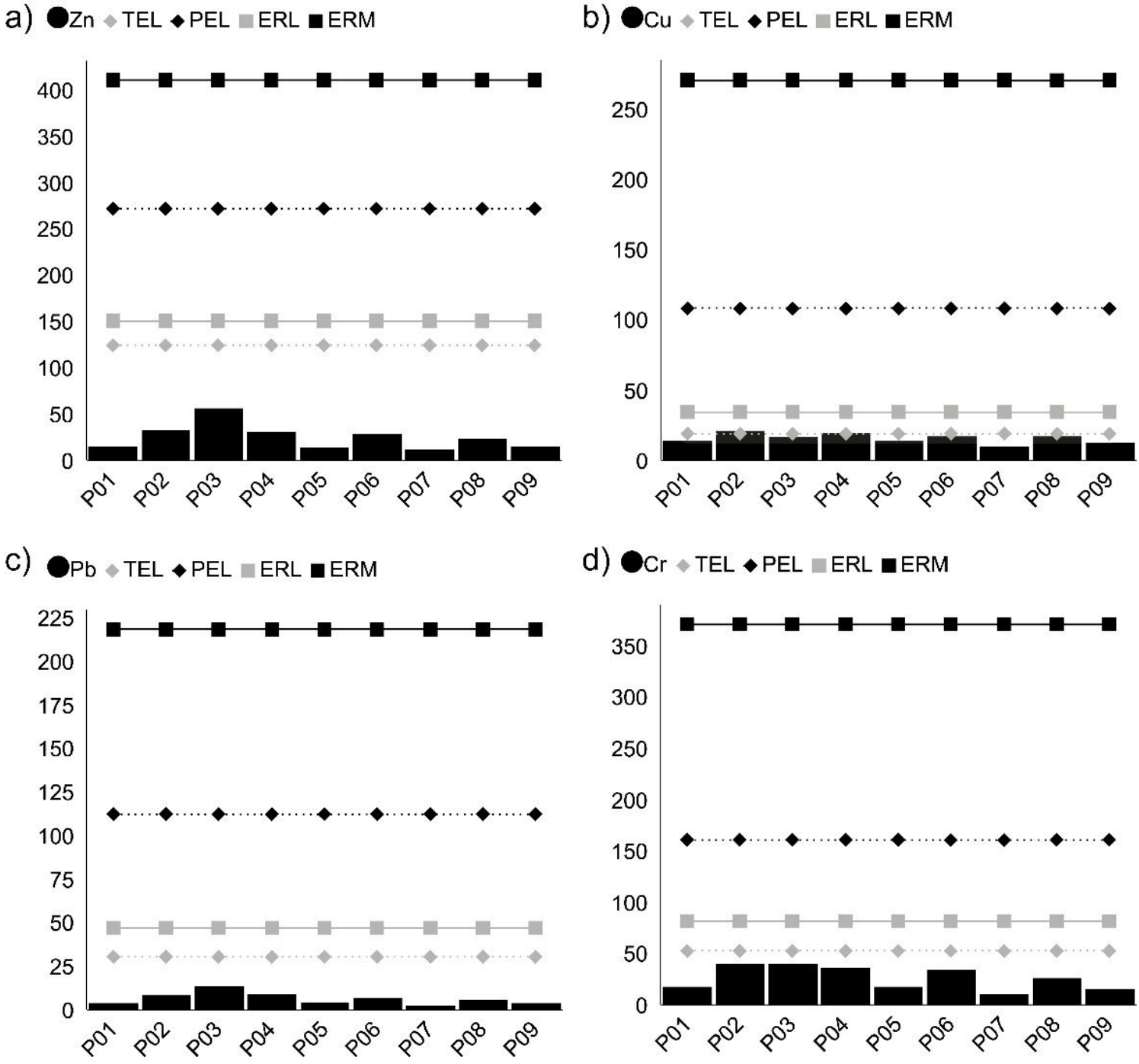

Figure 3

Concentrations of a) Zn, b) Cu, c) Pb and d) Cr (µg/g) compared to TEL, PEL, ERL and ERM values

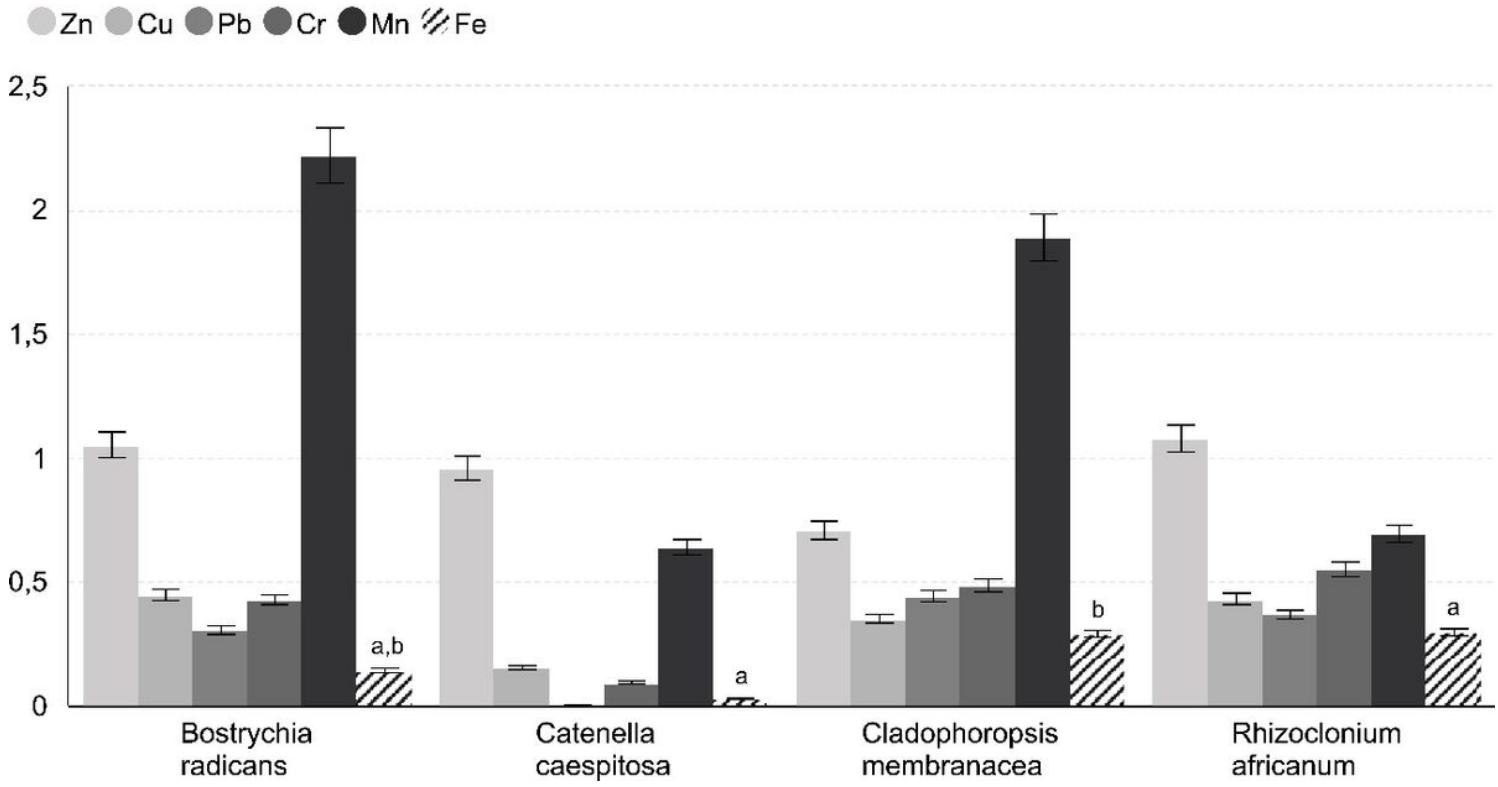

Figure 4

Bioconcentration Factor (BCF) for the species *B. radicans*, *C. membranacea*, *C. caespitosa* and *R. africanum* (mean ± standard error). Different letters indicate significant differences between Fe values in macroalgae according to Tukey's Post-Hoc test ($p < 0.05$)

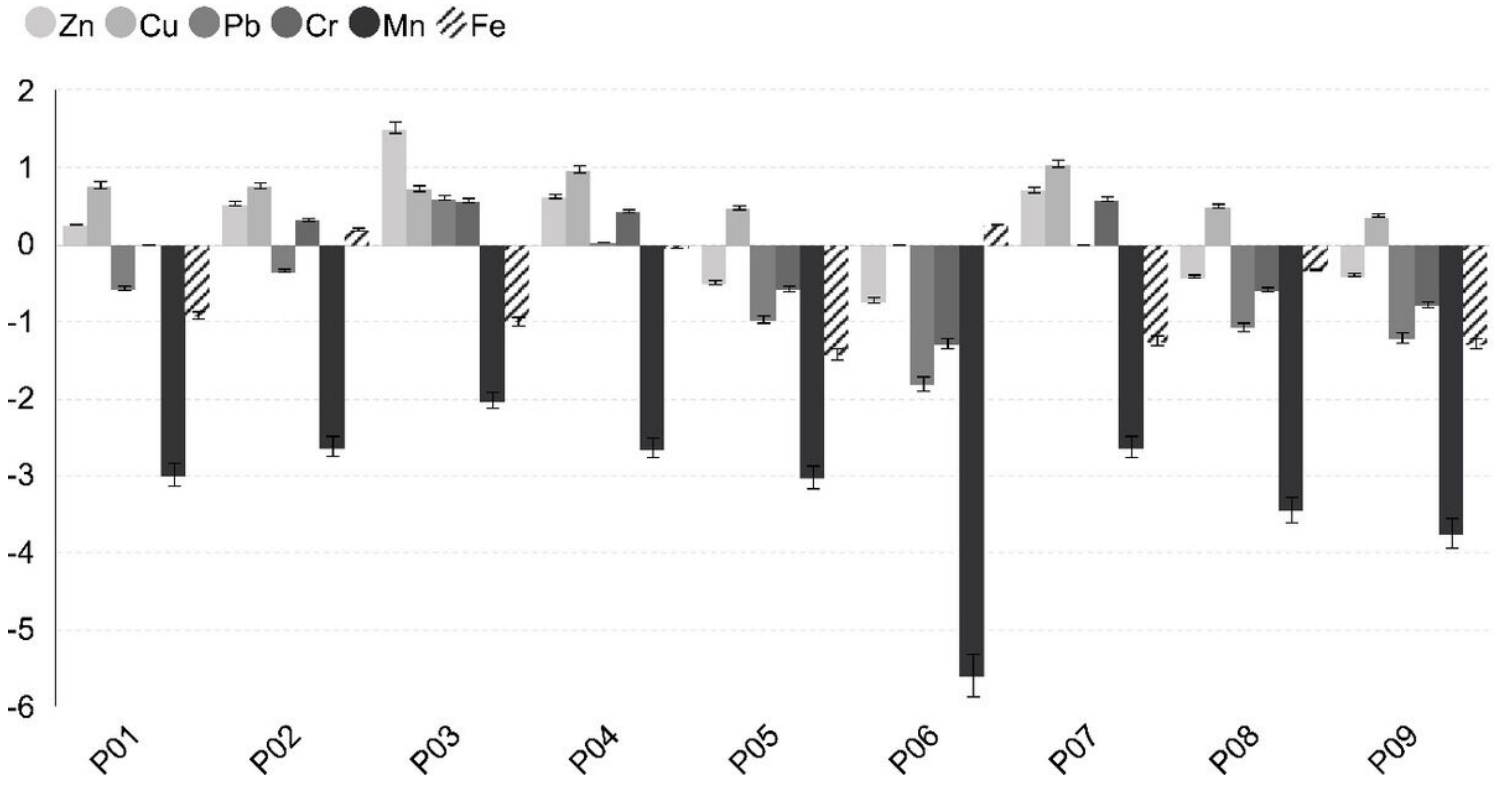

Figure 5

Geoaccumulation Index (Igeo) for all collection points (mean ± standard error) of the mangroves of São Luís Island, Maranhão

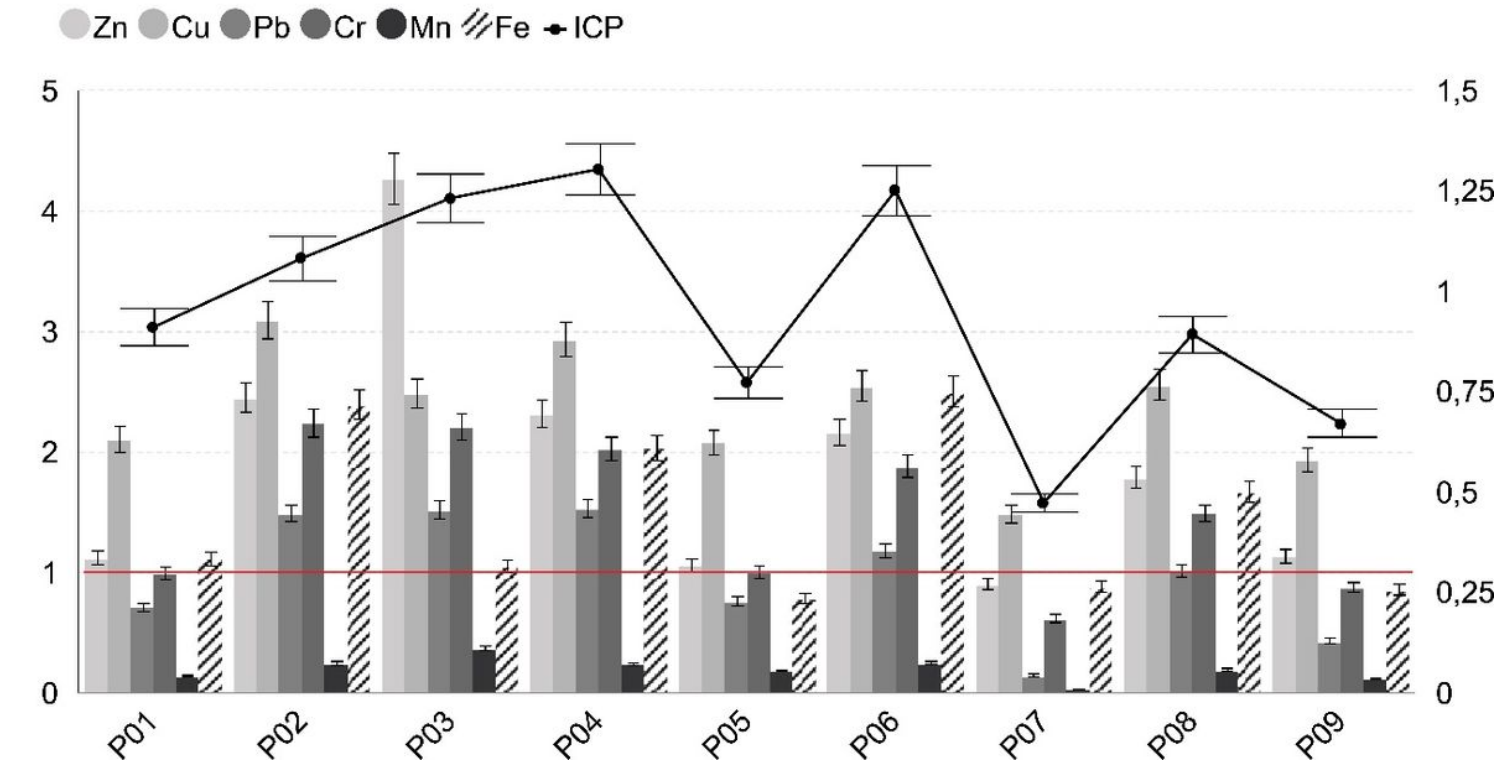

Figure 6

Contamination Factor (bars) and Pollutant Load Index (line) for all collection points (mean ± standard error). Red line indicates the threshold above which environments tend to be moderately contaminated

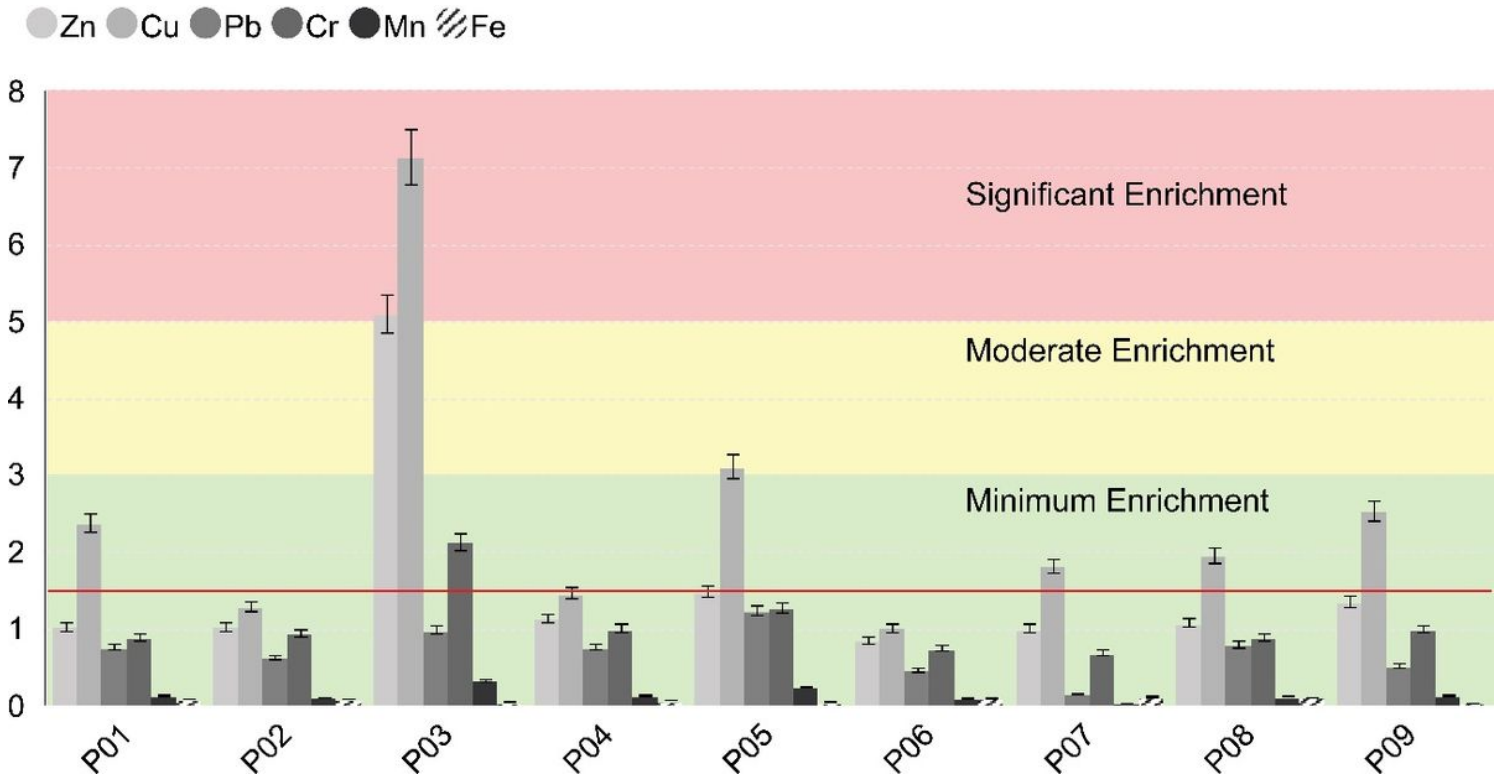

Figure 7

Enrichment Factor (EF) for all collection points (mean + standard error). Red line indicates the limit above which mineral enrichment has anthropogenic influence